Multiplex Microfluidic Paper-based Immunoassay for the Diagnosis of Hepatitis C Virus Infection

ARTICLE *in* ANALYTICAL CHEMISTRY · MAY 2014

Impact Factor: 5.64 · DOI: 10.1021/ac500247f · Source: PubMed

5 AUTHORS, INCLUDING:

Xuan Mu
Chinese Academy of Medical Sciences
15 PUBLICATIONS **203** CITATIONS
SEE PROFILE

Lin Zhang
University of Melbourne
13 PUBLICATIONS **44** CITATIONS
SEE PROFILE

analytical chemistry

Article

pubs.acs.org/ac

Multiplex Microfluidic Paper-based Immunoassay for the Diagnosis of Hepatitis C Virus Infection

Xuan Mu,*[,†] Lin Zhang,[‡] Shaoying Chang,[†] Wei Cui,[‡] and Zhi Zheng*[,†]

[†]Institute of Basic Medical Sciences, Chinese Academy of Medical Sciences, School of Basic Medicine, Peking Union Medical College, 5 Dongdan Santiao Beijing, 100005 P. R. China

[‡]Department of Laboratory Medicine, Peking Union Medical College Hospital, Chinese Academy of Medical Sciences, and Peking Union Medical College, 1 Shuaifuyuan Beijing, 100730 P. R. China

S *Supporting Information*

ABSTRACT: Hepatitis C virus (HCV) infection is a serious and rising global healthcare problem. One critical challenge to tackle this disease is the lack of adequate diagnosis. Here, we develop a multiplex microfluidic paper-based immunoassay, as a novel diagnostic approach, to detect human IgG antibody against HCV (anti-HCV). The paper substrate, highly flammable nitrocellulose (NC), is patterned under ambient temperature by craft punch patterning (CPP) to generate multiple test zones. On the basis of superior merits of patterned paper, this new diagnostic approach demonstrates the key novelty to unprecedentedly combine segmented diagnostic assays into a single multiplex test. The generated diagnostic results are not only informative but can be rapidly and cost-effectively delivered. It would significantly transform the clinical pathway for unwitting individuals with HCV infection. This work highlights the promising role of microfluidic paper-based immunoassays in tackling the diagnostic challenge for the HCV pandemic as well as other diseases.

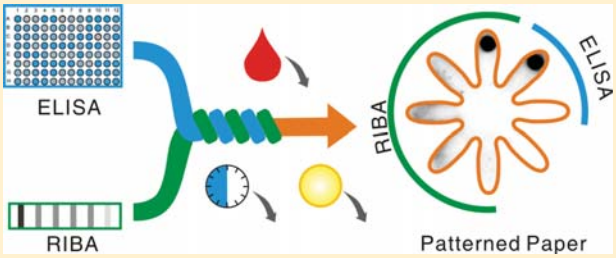

Hepatitis C virus (HCV) is the principle cause of liver cirrhosis and hepatocellular carcinoma, accounting for more deaths than HIV in the United States (U.S.) and infecting an estimated 150 million people worldwide.[1,2] Although this chronic infectious disease is one of the most serious global healthcare issues with growing impact in the next decade,[3] its real magnitude remains elusive, even referred to as a "silent pandemic."[4,5] A majority of infected individuals are just out of the reach of diagnosis.[4,5] For example, even in the U.K. and U.S., only 25% and 50% of patients, respectively, get a confirmed diagnostic result.[6,7] Unwitting virus carriers would expedite the spread of the disease and suffer from end-stage conditions that are intractable and cause huge expenditures. Additionally, over tens of millions of individual (such as baby boomers), as recommended by the U.S. Centers for Disease Control and Prevention (CDC), should receive routine HCV testing.[7] The critical challenge of inadequate diagnosis particularly in a large population at risk desperately needs to be addressed.

The deficiency of diagnosis is, in part, related to a conventional diagnostic approach that is segmented into at least two steps. The first step, as a first-line diagnosis, is usually the serologic detection of IgG antibody against HCV (anti-HCV) by enzyme-linked immunosorbent assay (ELISA).[8] ELISA employs a pool of epitopes to gain a relatively high sensitivity, but so many epitopes would capture noncorresponding antibodies as well, decreasing specificity and tending to generate false-positive results, especially for low-prevalence populations.[9,10]

As requested by CDC, the second assay is imperative to circumvent the false-positive bias of ELISA and confirm the diagnostic result,[11,12] such as recombinant immunoblot assay (RIBA). It is also a serologic immunoassay for IgG antibody but employs multiple individual antigens to report a reaction pattern, thus inherently providing a higher level of specificity than ELISA.[13,14] However, its routine utilization might be hampered by high cost (at least 2-fold that of ELISA), low sensitivity, and long assay time (6−7 h).[15] Most importantly, the segmented clinical pathway itself might be a major reason to hinder the effective delivery of diagnosis by adding diagnostic complexity, delaying turnaround time and increasing office visits.

Recently, microfluidic paper-based analytical devices (μPAD)[16−18] have demonstrated huge potential to transform conventional immunoassays for clinical diagnosis and healthcare monitoring.[19−24] The utilization of paper as an emerging substrate material in microfluidics[25−27] would offer exceptional merits. The paper substrate is much less expensive than a plastic well plate, and its intrinsic capillary force could move liquids, eliminating the need of external power sources and pumps. The high surface-to-volume ratio of paper due to its

Received: January 20, 2014
Accepted: May 5, 2014
Published: May 5, 2014

dx.doi.org/10.1021/ac500247f | *Anal. Chem.* 2014, 86, 5338−5344

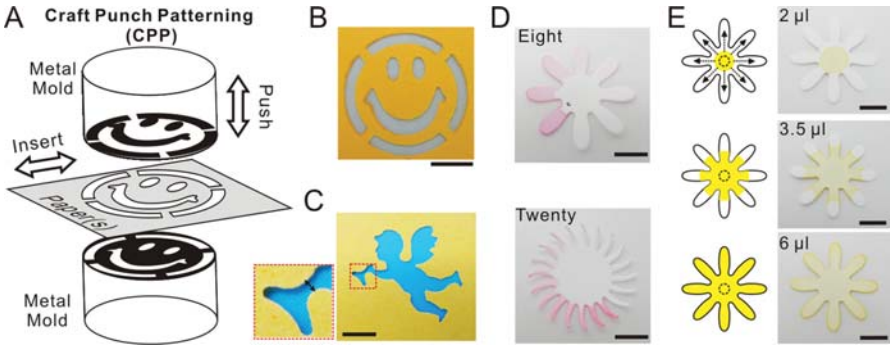

Figure 1. Schematics and photo images of craft punch patterning (CPP). (A) Schematics of the convenient patterning procedure using a craft punch: inserting paper(s) and pushing button. (B) The corresponding photo image of the patterned smiley-face on colored paper. (C) The photo image of a patterned flying cherub holding a horn. The smallest feature, indicated by black arrows, is about 400 μm. (D) Two patterned NC membranes of 16 mm diameter for multiplex assays. The detection zones (about 5 mm^2) in petals are marked by a series of diluted red dye solutions. (E) Schematics and photo images of introducing a sample at the center (indicated by dash circle). The liquid can be spontaneously delivered outward indicated by the dashed arrows. The numbers at the upper left indicate the volume of pipetted liquid. Scale bars represent 5 mm.

fibrous nature would dramatically diminish the diffusion distance and time, benefiting capture and binding.[20] Moreover, one distinctive feature of μPAD is patterned structure.[28−33] It is advantageous as it allows the deliberate manipulation of fluid flows for complex functions, such as automated multistep processes[34−38] and multiplex assays.[39] However, most patterning methods involving a temperature over 100 °C may be restricted to patterning highly flammable materials like nitrocellulose (NC).[40,41] A patterning method under ambient temperature is of special interest and is still in demand.

In this paper, we harness the irreplaceable merits of multiplex microfluidic paper-based immunoassay to integrate the lengthy, costly, and segmented assays in a rapid and economic manner, which shows great potential to transform the diagnostic pathway for confronting the HCV pandemic.

EXPERIMENTAL SECTION

Materials. The craft punch was purchased from Jufeng Metal Plastic Inc. (Jef, Dongguan, Guangdong, China). Nitrocellulose membrane Protran (a pore size of BA83 and BA85 is 0.2 and 0.45 μm, respectively) and chromatography paper (Grade 1 Chr) were bought from Whatman and Amersham, GE Healthcare (U.S.). Bovine Serum Albumin (BSA, A2058), HRP-labeled anti-Human IgG (A8792), Anti-Human IgG antibody (SAB3701331), 3,3′,5,5′-tetramethylbenzidine (TMB, T0565), and mouse IgG (I5381) were obtained from Sigma-Aldrich (U.S.). Immobilon Western Chemiluminescent Substrate for HRP (WBKLS0500) was bought from Millipore (U.S.). HRP-labeled anti-Mouse IgG (7076) was bought from CST. HCV antigens including Core protein (40 kDa, ab43027), NS4 (33 kDa, ab67978), and NS5 (38 kDa, ab68616) were bought from abcam (U.S.). These antigens, as reported in datasheets, are immunoreactive with sera of HCV-infected individuals. We bought a China-FDA approved commercial anti-HCV ELISA kit (01010808023) from Beijing Chemclin Biotech Co. (Beijing, China). It includes an antigen-coated 96-well plate, positive and negative control serums, serum dilute buffer, wash buffer, HRP-labeled antihuman IgG solution, and HRP substrates. Besides positive and negative control serums, other components in the kit were only used for 96-well ELISA.

Ten units of patient serum were obtained from the Department of Laboratory Medicine, Peking Union Medical College Hospital with ethical review and approval. A panel of four reference serums for evaluating detection sensitivity was obtained from National Center for Clinical Laboratories (China).

The Procedure of Patterning Paper. The paper was manually patterned by craft punch patterning (CPP) in a die-cast mechanism under ambient temperature. CPP avoids a temperature over 100 °C that is especially harmful for patterning highly flammable paper like NC. The manipulation of patterned paper needs forceps that are blunt and should avoid direct contact with fingers.

The Procedure of Immunoassay on Patterned Paper. The antigen or antibody was diluted in phosphate buffer saline (PBS, pH = 7.4) to specific concentrations. The prepared solutions (0.5 μL) were pipetted on each detection zone of patterned paper. The paper was allowed to dry in the air for 30 min, followed by blocking in PBS containing 5% BSA and 0.05% Tween-20 for 60 min. If not used immediately, the blocked paper could be stored at 4 °C for at least weeks. According to the manufacturer, Protran NC should be stored in a clean, dry atmosphere away from noxious fumes, avoiding conditions of extreme humidity and exposure to sunlight. The proper storage could ensure the molecular recognition capability of immobilized proteins for years, which is a unique benefit for extending the shelf life of NC-based diagnostic products.

For detecting mouse IgG, the blocked paper was immersed in the solution of HRP-labeled anti-Mouse IgG (1:5000) for 5 min, followed by washing three times in PBS (pH = 7.4) containing 0.05% Tween-20, each for 2 min, in a 3D gyratory rocker (SSM3, Stuart, UK).

For detecting anti-HCV, 0.3 μL of the positive and negative controls and diluted patient serum was pipetted on blocked detection zones for 1 min, followed by washing (as above). The patient serum was diluted (1:50) in PBS containing 10% BSA. The patterned paper was then incubated in the solution of HRP-labeled antihuman IgG (1:50000) for 2 min and washed (as above). After washing enzyme-labeled antibodies away, 250 μL of newly mixed chemiluminescence substrate was gently poured onto the patterned paper. After 1 min, most of liquids were aspirated out followed by detection.

Image Capture and Analysis. Chemiluminescence of the commercial ELISA kit was detected in a Modulus Microplate

dx.doi.org/10.1021/ac500247f | Anal. Chem. 2014, 86, 5338−5344

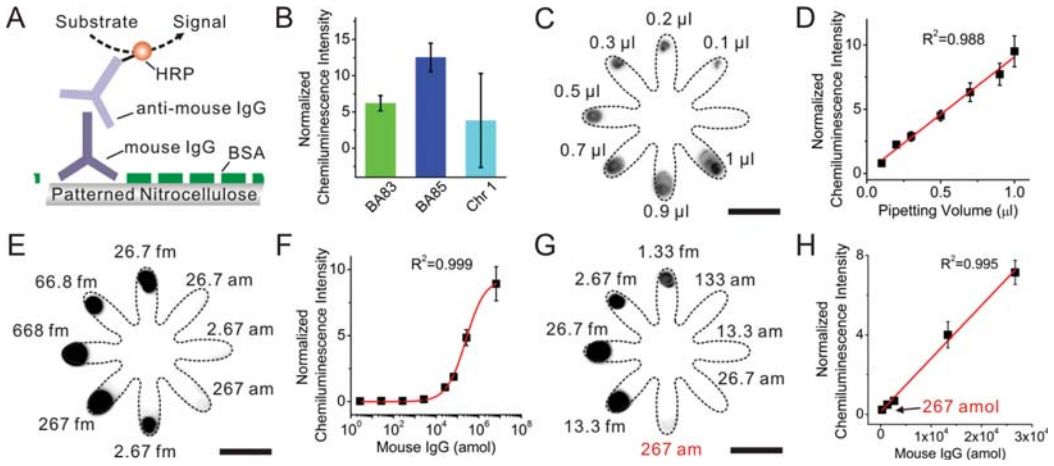

Figure 2. Indirect-ELISA on patterned NC for quantitatively detecting mouse IgG. (A) Schematics of indirect ELISA procedures. The labeled horseradish peroxidase (HRP) could catalyze the substrate and generate signals including chemiluminescence and color precipitates. (B) The comparison of chemiluminescence signals of 1 μg/mL mouse IgG on Protran BA83 and BA85 and Chr 1. Protran BA85 is preferential for immobilizing proteins over 20 kDa and thus shows higher signal than others. (C and D) Chemiluminescence image and plot of different pipetting volumes of mouse IgG that shows a linear relationship (R^2 = 0.988). (E and F) Chemiluminescence image and plot of mouse IgG from 668 fmol (200 μg/mL) to 2.67 amol (0.8 ng/mL) that is fitted well with the Hill equation (R^2 = 0.999). (G and H) Chemiluminescence image and plot of mouse IgG from 26.7 fmol (8 μg/mL) to 13.3 amol (4 ng/mL). The chemiluminescence intensity from 26.7 fmol to 267 amol (80 ng/mL) is linear (R^2 = 0.995). The limit of quantification (LOQ) is 267 amol. The pipetting volume per each detection zone in E, F, G, and H is 0.5 μL. Dashed lines indicate the boundary of patterned paper. Each datum is the average of three measurements, and the error bars represent the standard deviation. The fm and am indicate fmol and amol, respectively. Scale bars represent 5 mm.

Multimode Reader (Turner Biosystems, US) in accordance with the procedure provided by the manufacture. The chemiluminescence on patterned paper was captured in an ImageQuant Las 4000 mini (GE Healthcare, US) for 15 min. The colorimetric image of patterned paper was captured by a Digital Camera. All the images gained in experiments were analyzed in ImageJ (NIH, US). The color intensity was measured in a uniform circle at each detection zone. For the image in RGB format, it was converted into 8-bit grayscale before quantitative analysis. The signal data were normalized by subtracting background signal at the center of patterned paper.

RESULTS AND DISCUSSION

Craft Punch Patterning. Patterning paper is an essential step toward fulfilling analytical purposes. Specific properties of the paper substrate would add useful functions as well as impose strict requirements on patterning methods. Because nitrocellulose (NC) shows outstanding capacity for immobilizing proteins via noncovalent hydrophobic forces,[42] it has been widely used for qualitative and quantitative detection of proteins in Western blot, dot blot, and lateral flow immunoassays for several decades.[43,44] However, NC is combustible in air (decompose at 55 °C and undergo autoignition at 130 °C).[40] Such vulnerability of NC makes it worrisome and troublesome to utilize most of the patterning methods,[41] such as photolithography (baking SU-8 at 95 °C),[28] wax printing (baking wax at 125 °C)[29,30] and laser cutting.[45]

To circumvent this issue, we developed a new patterning method called craft punch patterning (CPP). While the craft punch is a vigorous tool in paper handicraft,[46] we assumed it to be equally useful in patterning paper for analytical purposes. A craft punch contains one pair of interacting metal molds that have intermesh structures (Figures 1A and S1). It can pattern papers in a die-cast manner and, notably, under ambient temperature. Therefore, CPP avoids a temperature inappropriate for NC, which not only eliminates the worry of ignition but also maintains the natural microstructure of NC that is useful to immobilization and detection of proteins.

The operation of CPP is to insert paper(s) followed by pushing button, which is rapid, simple, and convenient for untrained personnel. We demonstrated the capability of CPP by patterning a well-known smiley-face (Figure 1B) and a more complex shape, a flying cherub holding a horn (Figure 1C), on colored papers. The inset image indicates the smooth curve boundary and precision (about 400 μm) of the pattern, which is comparable to or better than other prototyping patterning methods.[47,48] The geometry of the pattern could be versatile because of hundreds of different off-the-shelf craft punches and metal molds. In addition, a craft punch is inexpensive (less than U.S. $2) and has the potential to form an array by assembling many craft punches for parallel fabrication. Due to its ambient operation, precision, convenience, versatility, and potential for massive fabrication, CPP is fairly applicable to patterning highly flammable paper like NC and should be a compelling alternative to other patterning methods like a computer-controlled knife.[49]

To develop a multiplex immunoassay on paper, we adopted CPP to pattern NC in a flower-like shape (Figure 1D and E). The patterned NC paper is only 16 mm in diameter, smaller than a quarter dollar coin. The "petals" could serve as multiple detection zones, and the radial shape would utilize air barriers between detection zones to prevent from cross contamination. When implementing assays, we could pipet liquids either directly on each detection zones, shown by a series of diluted solution of red dye (Figure 1D), or at the center as a sample inlet, from which liquid can be delivered by capillary force into surrounding detection zones (Figure 1E). Both methods could detect multiple targets in one sample, while the former consumes fewer samples and the latter is less labor-intensive.

Quantitative Detection of Mouse IgG. To determine the analytical performance of the patterned NC, we performed an

dx.doi.org/10.1021/ac500247f | Anal. Chem. 2014, 86, 5338−5344

indirect-ELISA for quantitatively detecting mouse IgG through chemiluminescence (Figure 2A). Three categories of papers, including Chr 1 and Protran BA83 and BA85, demonstrate different detection results (Figure 2B). Chr 1 is pure cellulose useful for chromatography analysis but lacks functional groups for immobilizing proteins, therefore showing rather unstable signals and thus being infeasible for immunoassay (Figure 2B).[50] In comparison with Chr 1, Protran BA83 and BA85 are nitrocellulose papers that show higher and more stable results. Due to different pore sizes, BA83 and BA85 are usually suitable for immobilizing proteins below and above 20 kDa, respectively. Because the molecular weight of mouse IgG is approximately 150 kDa (larger than 20 kDa), BA85 is superior to BA83 to show a higher signal (Figure 2B).

The multiplex nature of a patterned NC (Figure 1D and E) could facilitate the optimization of assay procedures and the generation of a calibration curve. We pipetted a series of seven different volumes, ranging from 0.1 μL to 1 μL, of mouse IgG on the detection zones of a piece of patterned NC (Figure 2C). The volume of 0.1 μL could generate an observable signal, owing to the small area of detection zones (about 5 mm^2) and sufficient protein immobilization. The signal intensity, as expected, is linear to the pipetting volume (R^2 = 0.988; Figure 2D), demonstrating the reliable handling of minute liquids. The larger pipetting volume leads to a stronger signal, while it costs more samples and is more likely to cause cross-contaminations. We therefore chose compromising pipet volumes as 0.3 and 0.5 μL in the following experiments.

We obtained a calibration curve of mouse IgG from 668 fmol to 2.67 amol on patterned papers in one single test (Figure 2E). The data are fitted well with the nonlinear Hill equation with a correlation coefficient of 0.999 (Figure 2F). The equation describes a dynamic binding process of a ligand to a receptor like antigen to antibody.[20] Particularly, over the concentration range between 26.7 fmol and 267 amol (2 orders of magnitude), the chemiluminescence intensity is approximately linear with a correlation coefficient of 0.995 (Figure 2G and H). The limit of quantification (LOQ) is as low as 267 amol (~40 pg), which approaches the detection limit (LOD) of the employed substrate (~1 pg). It is worth noting that LOQ is usually higher than LOD, and the detection limit depends on many factors, including the substrate as well as the affinity between antibody and antigen, and the nonspecific binding of enzyme-labeled antibody.

To demonstrate the capability of colorimetric detection of mouse IgG on patterned NC, we employed a highly sensitive colorimetric substrate, insoluble TMB (detection limit, 0.15 ng) that would generate purple precipitation (Figure 3A). The visible precipitation is convenient for capturing via inexpensive imagers like a digital camera or a smart phone.[51,52] The colorimetric signal is processed into a normalized gray value that is linearly proportional to the concentration of mouse IgG from 668 fmol to 26.7 fmol with a correlation coefficient of 0.988 (Figure 3B). The LOQ is as low as 26.7 fmol (~4 ng), which is lower by half than a previous LOD (54 fmol of rabbit IgG).[20] To ensure such a low detection limit, rapid (≤2 min) and thorough washing (in a 3D gyratory rocker) is necessary to alleviate nonspecific binding that may be the primary deviation. We did not observe cross-contamination during washings. Although it may be a potential concern, excellent protein immobilization as well as a relatively large volume of washing solution (1000 μL) could effectively minimize its occurrence.

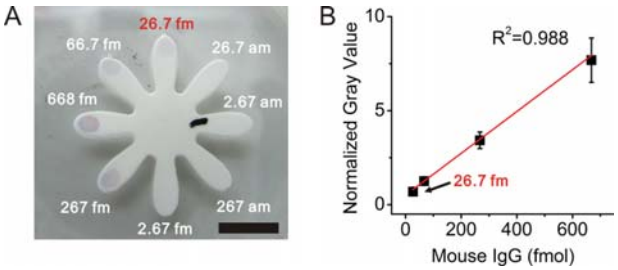

Figure 3. Colorimetric detection of mouse IgG on patterned NC. (A) Photo image of detecting mouse IgG via colorimetric substrate, insoluble TMB. One short black mark on the middle-right petal was for positioning. (B) The processed gray value shows a linear relationship between 668 fmol and 26.7 fmol (R^2 = 0.988). The limit of quantification (LOQ) is 26.7 fmol. Each datum is the average of three measurements, and the error bars represent the standard deviation. The fm and am indicate fmol and amol, respectively. Scale bar represents 5 mm.

Qualitative Detection of anti-HCV. On the basis of the quantitative detection of mouse IgG, we demonstrated the qualitative detection of anti-HCV by using an equal mixture of individual recombinant HCV antigens, including Core, NS4, and NS5. Figure 4A shows the schematics of the experimental procedure. Since the antigens are larger than 20 kDa, we continued to adopt Protran BA85 as the solid support for immunoassay.

Figure 4B shows the optimization of antigen concentration by analyzing a positive control serum (provided in the commercial ELISA kit). From 20 μg/mL to 100 μg/mL, the chemiluminescence signal increases as the antigen concentration rises. However, the signal at 200 μg/mL is lower than that at 100 μg/mL. The diminished signal may be due to the hook effect that describes the diminished binding sites caused by the interaction between excess immobilized proteins. The 100 μg/mL antigen in the mixture, therefore, is the optimum and employed in the following experiments.

Because the immunoassay for detecting anti-HCV is qualitative, its result is usually represented by a signal-to-cutoff (S/Co) ratio that is defined by the ratio of signals between tested serum and negative control serum (provided in the commercial ELISA kit). If the S/Co is larger than a threshold (2.1, provided by the ELISA kit), the test would be recognized as positive and vice versa. Figure 4C shows the results of a series of positive control serum dilutions and negative control serum. The S/Co of 100-diluted positive control serum is still higher than the threshold. In addition, we tested a panel of certified reference serums that are from weak to strong positive (Figure S2). The weakest positive serum demonstrates a S/Co (2.9) that is larger than 2.1. These results support the adequate sensitivity of a paper-based immunoassay for analyzing clinical serum.

Diagnosis of HCV Infection. Because ELISA and RIBA are similar in principle and procedures of serological immunoassays, it seems technically feasible to simultaneously perform them on different detection zones of one piece of patterned NC, as shown in Figure 4D. Two detection zones in the blue boundary, immobilized with the mixtures of recombinant antigens, could function as ELISA. Another five detection zones in the green boundary, immobilized with individual HCV antigens and human IgG antibody, could serve as RIBA. We employed this configuration for detecting anti-HCV in real

dx.doi.org/10.1021/ac500247f | Anal. Chem. 2014, 86, 5338−5344

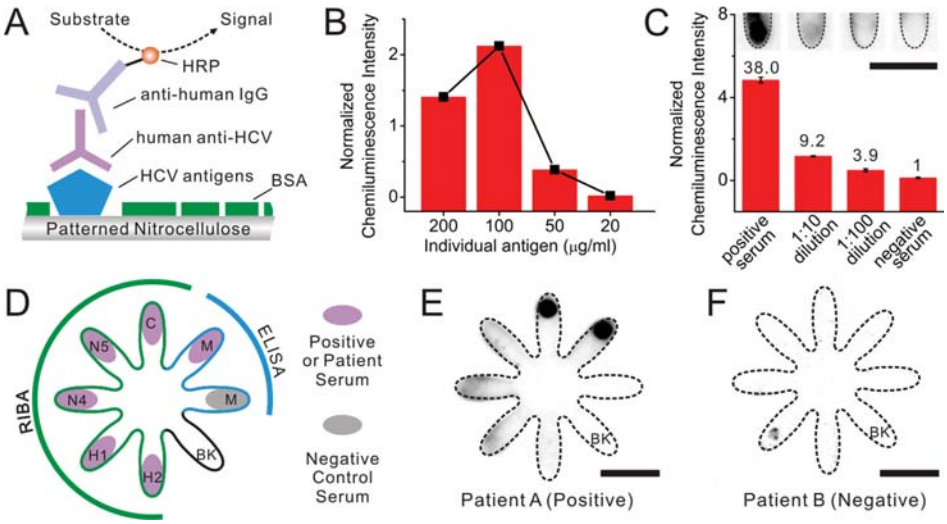

Figure 4. Multiplex paper-based immunoassay for the detection of anti-HCV and HCV diagnosis. (A) Schematic illustration of assay procedures. The individual recombinant HCV antigens or the equal mixtures are immobilized on specific detection zones. (B) The 100 μg/mL of antigen concentration in the mixture shows the optimum signal. The hook effect may contribute to the diminished signal at 200 μg/mL. (C) Representative images (top) and corresponding bar chart (bottom) of positive control serum, its two dilutions, and negative control serum. The number indicates the S/Co ratio. The S/Co ratio of 100-fold dilution is above the threshold of 2.1 and distinguishable from negative control serum. (D) Schematic illustration of the combination of segmented ELISA and RIBA assays. The immobilized antigens were labeled (M for the mixture of antigens; C for Core; N5 and N4 for NS5 and NS4, respectively; H1 and H2 for human IgG antibody at 12 μg/mL and 6 μg/mL, respectively; BK for Blank). The human IgG antibody could capture human IgG in serums for positive control. (E and F) Representative chemiluminescence images of patient A and patient B. The images are analyzed and interpreted in Table 1. In both images, the signal of H2 is too weak to be visible. Each datum is the average of three measurements, and the error bars represent the standard deviation. Dash lines indicate the boundary of patterned paper. Scale bars represent 5 mm.

patient serums (Figure 4E and F and Table 1). Of note, the patient serum should be diluted at least 50-fold before pipetting on paper to eliminate false-positive results and background noise associated with a matrix effect.

Table 1. Multiplex Paper-Based Immunoassay for Anti-HCV in Patient Serums

	S/Co (2.1)[a]		reaction pattern (0.7)[c]				
serum	NC	ELISA[b]	Core	NS4	NS5	>0.7	results[d]
patient A	97.61	56.60	**6.91**	**0.90**	**1.71**	3	positive
patient B	0.30	0.19	0.16	0.11	0.33	0	negative
patient C	0.40	0.22	0.48	0.24	0.26	0	negative
patient D	26.24	14.1	**0.72**	**4.12**	0.67	2	positive
patient E	0.9	1.04	0.21	0.14	0.20	0	negative
patient F	1.5	1.13	0.19	0.20	0.63	0	negative
patient G	42.61	34.6	**5.57**	**1.69**	**1.58**	3	positive
patient H	0.76	0.83	0.18	0.11	0.17	0	negative

[a]S/Co = the signal to cutoff ratio. The threshold is shown in brackets. NC is nitrocellulose. [b]The results of the commercial ELISA kit. [c]The result is the ratio of signal to H1; a value larger than 0.7 is marked in bold and counted. [d]The diagnostic results of paper-based immunoassay and ELISA are consistent.

The S/Co ratio of three positive serums (A, D, and G) and five negative serums (B, C, E, F, and H) is larger and lower than the threshold (2.1), respectively. The diagnostic results of the paper-based immunoassay are consistent with that of a commercial ELISA kit (Table 1).

The result of individual antigen is represented by the ratio of signal to human IgG (H1) and forms a reaction pattern (Table 1). The reaction pattern of multiple individual antigens can elucidate the specificity of antibody response and confirm the results of ELISA through a threshold (0.7 for current results). For example, in positive serums, the result of more than two antigens is higher than 0.7. In negative serums, no antigen is higher than 0.7. We also tested two serums from patients with the hepatitis B virus (HBV) infection that is usually a coinfection with HCV. The negative results indicate the antigen specificity (Figure S3).

It is noteworthy that one antigen of HCV, NS3, was not employed in the current paper-based immunoassay. The adoption of NS3 in future assays would further improve the analytical performance of the paper-based HCV diagnosis.

Except for the same detection target of anti-HCV, ELISA and RIBA have distinctive and complementary functions relevant to the HCV diagnosis. The S/Co of ELISA could show close relevance and important value to the disease progress,[53] while the reaction pattern in RIBA would reveal the serotype of HCV[54] that is necessary to guide clinical treatment. Therefore, the combination of ELISA and RIBA on a microfluidic paper-based immunoassay would be synergic to provide informative diagnostic results, underpinning a new diagnostic pathway.

The microfluidic paper-based immunoassay demonstrates remarkable miniaturization-associated merits (Table S1). The total assay time of analyzing patient serum is just 30 min, half of that in ELISA and one-twelfth of that in RIBA. It might be more rapid if adopting assisting methods like a vacuum.[55] Additionally, the material cost of one detection zone in a multiplex paper-based immunoassay is approximately estimated to be one-twenty-fifth of one well in 96-well ELISA (Table S2). Such a low material cost would establish an economic foundation for the practical implementation of combined assays as well as more complicated multiplex assays.

dx.doi.org/10.1021/ac500247f | Anal. Chem. 2014, 86, 5338−5344

More striking is the required serum that is as low as 6 nL per detection zone, where 0.3 μL of the 50-diluted serum is pipetted, approximately 2000 times lower than 10 and 20 μL serum in ELISA and RIBA, respectively. Such a low serum volume would be particularly useful when clinical samples are limited and multiple targets need to be detected. It also enables the replacement of venipuncture with a finger stick that is less invasive to the patient and more convenient to implement. Not only do the dramatically reduced assay time, material cost, and serum, due to the features of patterned paper, strengthen the feasibility of combining ELISA and RIBA assays, but these merits also show great capability to make HCV diagnosis more accessible and deliverable.

CONCLUSION

In conclusion, we developed a multiplex microfluidic paper-based immunoassay for addressing the diagnostic challenge for HCV infection. Since the solid phase of immunoassay is highly flammable NC, a new patterning method, CPP, is proposed to eliminate the worry of autoignition. In a paper-based immunoassay, the LOQ of mouse IgG is determined to be as low as 267 amol and 26.7 fmol in chemiluminescence and colorimetry, respectively. Because the detection is based on conventional HRP-chemiluminescence, the assay sensitivity would be further improved by adopting new amplification and labeling techniques.[56−58]

The unique characteristics of patterned paper beneficially contribute to the remarkable reduction of serum volume, assay time, and material cost. Furthermore, it enables the unprecedented combination of segmented serological immunoassays, fittingly streamlining the complex clinical pathway of HCV infection. The combined immunoassay shows the compelling capability to substitute the conventional first-line diagnosis for HCV infection (ELISA) and provide highly informative diagnostic results to benefit the large number of unwitting carriers.[4,5] Of note, it also implicates a diagnostic perspective in devising new strategies to fight against the HCV pandemic. The microfluidic paper-based immunoassay would hold great potential to be useful in other clinical diagnoses, such as the detection of a biomarker panel (tens of proteins) of cancer and Alzheimer's disease.[59]

ASSOCIATED CONTENT

Supporting Information

Additional experimental results of HBV and reference serum, the comparison with ELSIA and RIBA, and the cost estimation. This material is available free of charge via the Internet at http://pubs.acs.org.

AUTHOR INFORMATION

Corresponding Authors

*Tel.: 86-10-69156952. E-mail: muxuan2008@gmail.com.
*Tel.: 86-10-69156951. E-mail: zhizheng10@yahoo.com.

Notes

The authors declare no competing financial interest.

ACKNOWLEDGMENTS

The authors gratefully appreciate the support from National Scientific and Technological Major Project of China (2013ZX09507005), National Natural Science Foundation of China (21305162, 21375119 and 81271926), as well as the kind help from Dr. Zhengguang Guo, Zhaozhen Sun and Zhikai Cheng.

REFERENCES

(1) Poynard, T.; Yuen, M. F.; Ratziu, V.; Lai, C. L. *Lancet* **2003**, *362*, 2095−2100.
(2) Ghany, M. G.; Strader, D. B.; Thomas, D. L.; Seeff, L. B. *Hepatology* **2009**, *49*, 1335−1374.
(3) Kershenobich, D.; Razavi, H. A.; Cooper, C. L.; Alberti, A.; Dusheiko, G. M.; Pol, S.; Zuckerman, E.; Koike, K.; Han, K. H.; Wallace, C. M.; Zeuzem, S.; Negro, F. *Liver Int.* **2011**, *31*, 4−17.
(4) Editorial: *Lancet* **2013**, *381*, 178.
(5) *The silent pandemic: Tackling hepatitis C with policy innovation*; Economist Intelligence Unit: London, 2012.
(6) Irving, W. L.; Smith, S.; Cater, R.; Pugh, S.; Neal, K. R.; Coupland, C. A. C.; Ryder, S. D.; Thomson, B. J.; Pringle, M.; Bicknell, M.; Hippisley-Cox, J. *J. Viral Hepatitis* **2006**, *13*, 264−271.
(7) *Morbidity and Mortality Weekly Report*; United States Centers for Disease Control and Prevention: Atlanta, GA, 2013; Vol. *62*, pp 362−365.
(8) Kwon, J. A.; Lee, H.; Lee, K. N.; Chae, K.; Lee, S.; Lee, D. K.; Kim, S. *Clin. Chem.* **2008**, *54*, 424−428.
(9) Dufour, D. R.; Talastas, M.; Fernandez, M. D. A.; Harris, B.; Strader, D. B.; Seeff, L. B. *Clin. Chem.* **2003**, *49*, 479−486.
(10) Kamili, S.; Drobeniuc, J.; Araujo, A. C.; Hayden, T. M. *Clin. Infect. Dis.* **2012**, *55*, S43−S48.
(11) Kiely, P.; Walker, K.; Parker, S.; Cheng, A. *Transfusion* **2010**, *50*, 1344−1351.
(12) Lai, K. K. Y.; Jin, M.; Yuan, S.; Larson, M. F.; Dominitz, J. A.; Bankson, D. D. *Clin. Chem.* **2011**, *57*, 1050−1056.
(13) Siman-Tov, D. D.; Zemel, R.; Kaspa, R. T.; Gershoni, J. M. *Anal. Biochem.* **2013**, *432*, 63−70.
(14) Wu, S. J.; Liu, Y. L.; Cheng, L. M.; Yin, B. T.; Peng, J.; Sun, Z. Y. *J. Med. Virol.* **2011**, *83*, 1930−1937.
(15) Kamili, S.; Drobeniuc, J.; Araujo, A. C.; Hayden, T. M. *Clin. Infect. Dis.* **2012**, *55*, S43−S48.
(16) Martinez, A. W.; Phillips, S. T.; Whitesides, G. M. *Proc. Natl. Acad. Sci. U. S. A.* **2008**, *105*, 19606−19611.
(17) Pollock, N. R.; Rolland, J. P.; Kumar, S.; Beattie, P. D.; Jain, S.; Noubary, F.; Wong, V. L.; Pohlmann, R. A.; Ryan, U. S.; Whitesides, G. M. *Sci. Transl. Med.* **2012**, *4*, 152−129.
(18) Mu, X.; Zheng, W.; Sun, J.; Zhang, W.; Jiang, X. *Small* **2013**, *9*, 9−21.
(19) Wang, P. P.; Ge, L.; Yan, M.; Song, X. R.; Ge, S. G.; Yu, J. H. *Biosens. Bioelectron.* **2012**, *32*, 238−243.
(20) Cheng, C. M.; Martinez, A. W.; Gong, J. L.; Mace, C. R.; Phillips, S. T.; Carrilho, E.; Mirica, K. A.; Whitesides, G. M. *Angew. Chem., Int. Ed.* **2010**, *49*, 4771−4774.
(21) Wang, S. M.; Ge, L.; Song, X. R.; Yu, J. H.; Ge, S. G.; Huang, J. D.; Zeng, F. *Biosens. Bioelectron.* **2012**, *31*, 212−218.
(22) Tian, J. F.; Li, X.; Shen, W. *Lab Chip* **2011**, *11*, 2869−2875.
(23) Bai, P.; Luo, Y.; Li, Y.; Yu, X. D.; Chen, H. Y. *Chin. J. Anal. Chem.* **2013**, *41*, 20−24.
(24) Sackmann, E. K.; Fulton, A. L.; Beebe, D. J. *Nature* **2014**, *507*, 181−189.
(25) Pelton, R. *TrAC, Trends Anal. Chem.* **2009**, *28*, 925−942.
(26) Ren, K.; Chen, Y.; Wu, H. *Curr. Opin. Biotechnol.* **2014**, *25*, 78−85.
(27) Ren, K.; Zhou, J.; Wu, H. *Acc. Chem. Res.* **2013**, *46*, 2396−2406.
(28) He, Q. H.; Ma, C. C.; Hu, X. Q.; Chen, H. W. *Anal. Chem.* **2013**, *85*, 1327−1331.
(29) Carrilho, E.; Martinez, A. W.; Whitesides, G. M. *Anal. Chem.* **2009**, *81*, 7091−7095.
(30) Lu, Y.; Shi, W. W.; Qin, J. H.; Lin, B. C. *Anal. Chem.* **2010**, *82*, 329−335.
(31) Nie, J.; Liang, Y.; Zhang, Y.; Le, S.; Li, D.; Zhang, S. *Analyst* **2013**, *138*, 671−676.
(32) Bruzewicz, D. A.; Reches, M.; Whitesides, G. M. *Anal. Chem.* **2008**, *80*, 3387−3392.

(33) Fang, X.; Chen, H.; Jiang, X.; Kong, J. *Anal. Chem.* **2011**, *83*, 3596−3599.
(34) Fu, E.; Liang, T.; Spicar-Mihalic, P.; Houghtaling, J.; Ramachandran, S.; Yager, P. *Anal. Chem.* **2012**, *84*, 4574−4579.
(35) Apilux, A.; Ukita, Y.; Chikae, M.; Chailapakul, O.; Takamura, Y. *Lab Chip* **2013**, *13*, 126−135.
(36) Houghtaling, J.; Liang, T.; Thiessen, G.; Fu, E. *Anal. Chem.* **2013**, *85*, 11201−11204.
(37) Toley, B. J.; McKenzie, B.; Liang, T.; Buser, J. R.; Yager, P.; Fu, E. *Anal. Chem.* **2013**, *85*, 11545−11552.
(38) Lutz, B.; Liang, T.; Fu, E.; Ramachandran, S.; Kauffman, P.; Yager, P. *Lab Chip* **2013**, *13*, 2840−2847.
(39) Vella, S. J.; Beattie, P.; Cademartiri, R.; Laromaine, A.; Martinez, A. W.; Phillips, S. T.; Mirica, K. A.; Whitesides, G. M. *Anal. Chem.* **2012**, *84*, 2883−2891.
(40) *Millistak+ HC Filter Devices (with RW01)*; Millipore Corporation: Billerica, MA, 2008.
(41) Credou, J.; Volland, H.; Dano, J.; Berthelot, T. *J. Mater. Chem. B* **2013**, *1*, 3277−3286.
(42) MacPhee, D. J. *J. Pharmacol. Toxicol. Methods* **2010**, *61*, 171−177.
(43) Wong, R.; Tse, H. *Lateral Flow Immunoassay*; Humana Press: New York, 2009.
(44) Fridley, G. E.; Holstein, C. A.; Oza, S. B.; Yager, P. *MRS Bull.* **2013**, *38*, 326−330.
(45) Spicar-Mihalic, P.; Toley, B.; Houghtaling, J.; Liang, T.; Yager, P.; Fu, E. *J. Micromech. Microeng.* **2013**, *23*, 067003.
(46) U.S. Patent: US 2003/0213838 A1, 2003.
(47) Cheng, C. M.; Mazzeo, A. D.; Gong, J. L.; Martinez, A. W.; Phillips, S. T.; Jain, N.; Whitesides, G. M. *Lab Chip* **2010**, *10*, 3201−3205.
(48) Nie, J.; Zhang, Y.; Lin, L.; Zhou, C.; Li, S.; Zhang, L.; Li, J. *Anal. Chem.* **2012**, *84*, 6331−6335.
(49) Fenton, E. M.; Mascarenas, M. R.; Lopez, G. P.; Sibbett, S. S. *ACS Appl. Mater. Interfaces* **2009**, *1*, 124−129.
(50) Jarujamrus, P.; Tian, J. F.; Li, X.; Siripinyanond, A.; Shiowatana, J.; Shen, W. *Analyst* **2012**, *137*, 2205−2210.
(51) Martinez, A. W.; Phillips, S. T.; Carrilho, E.; Thomas, S. W.; Sindi, H.; Whitesides, G. M. *Anal. Chem.* **2008**, *80*, 3699−3707.
(52) Mu, X.; Tian, X. L.; Xu, K. F.; Zheng, Z. *Clin. Chem.* **2013**, *59*, A181.
(53) Takaki, A.; Wiese, M.; Maertens, G.; Depla, E.; Seifert, U.; Liebetrau, A.; Miller, J. L.; Manns, M. P.; Rehermann, B. *Nat. Med.* **2000**, *6*, 578−582.
(54) Gault, E.; Soussan, P.; Morice, Y.; Sanders, L.; Berrada, A.; Rogers, B.; Deny, P. *J. Clin. Microbiol.* **2003**, *41*, 2084−2087.
(55) Liu, Y.; Yu, J.; Du, M.; Wang, W.; Zhang, W.; Wang, Z.; Jiang, X. *Biomed. Microdevices* **2012**, *14*, 17−23.
(56) Hayat, A.; Andreescu, S. *Anal. Chem.* **2013**, *85*, 10028−10032.
(57) Qi, H. L.; Qiu, X. Y.; Xie, D. P.; Ling, C.; Gao, Q.; Zhang, C. X. *Anal. Chem.* **2013**, *85*, 3886−3894.
(58) Zhang, Y.; Guo, Y.; Xianyu, Y.; Chen, W.; Zhao, Y.; Jiang, X. *Adv. Mater.* **2013**, *25*, 3802−3819.
(59) Ray, S.; Britschgi, M.; Herbert, C.; Takeda-Uchimura, Y.; Boxer, A.; Blennow, K.; Friedman, L. F.; Galasko, D. R.; Jutel, M.; Karydas, A. *Nat. Med.* **2007**, *13*, 1359−1362.